Synoptic-scale controls of fog and low clouds in the Namib Desert

Hendrik Andersen[1,2], Jan Cermak[1,2], Julia Fuchs[1,2], Peter Knippertz[1], Marco Gaetani[3,4],
Julian Quinting[1], Sebastian Sippel[5,6], and Roland Vogt[7]

[1]Karlsruhe Institute of Technology (KIT), Institute of Meteorology and Climate Research, Karlsruhe, Germany
[2]Karlsruhe Institute of Technology (KIT), Institute of Photogrammetry and Remote Sensing, Karlsruhe, Germany
[3]LISA/IPSL, CNRS, Université Paris Est Créteil, Université Paris, Créteil, France
[4]LATMOS/IPSL, CNRS, Sorbonne Université, Université Paris-Saclay, Paris, France
[5]ETH Zurich, Institute for Atmospheric and Climate Science, Zurich, Switzerland
[6]Norwegian Institute of Bioeconomy Research, Ås, Norway
[7]University of Basel, Department of Environmental Sciences, Basel, Switzerland

Correspondence: Hendrik Andersen (hendrik.andersen@kit.edu)

Abstract. Fog is a defining characteristic of the climate of the Namib Desert and its water and nutrient input are important for local ecosystems. In part due to sparse observation data, the local mechanisms that lead to fog occurrence in the Namib are not yet fully understood, and to date, potential synoptic-scale controls have not been investigated. In this study, a recently established 14-year data set of satellite observations of fog and low clouds in the central Namib is analyzed in conjunction with reanalysis data to identify typical synoptic-scale conditions associated with fog and low-cloud occurrence in the central Namib during two seasons that characterize seasonal fog variability. It is found that during both seasons, mean sea level pressure and geopotential height at 500 hPa differ significantly between fog/low-cloud and clear days, with patterns indicating seasonally different synoptic-scale disturbances on fog and low-cloud days: cut-off lows during September, October, and November, and breaking Rossby waves during April, May, and June. These regularly occurring disturbances increase the probability of fog and low-cloud occurrence in the central Namib in two main ways: 1) an anomalously dry free troposphere in the coastal region of the Namib leads to stronger longwave cooling, especially over the ocean, facilitating low-cloud formation, and 2) local wind systems are modulated, leading to an onshore anomaly of marine boundary-layer air masses. This is consistent with air mass backtrajectories and a principal component analysis of spatial wind patterns that point to advected marine boundary-layer air masses on fog and low-cloud days, whereas subsiding continental air masses dominate on clear days. Large-scale free-tropospheric moisture transport into southern Africa seems to be a key factor modulating the onshore advection of marine boundary-layer air masses during April, May, and June, as the associated increase in greenhouse gas warming and thus surface heating is observed to contribute to a continental heat low anomaly. A statistical model is trained to discriminate between fog/low-cloud and clear days based on large-scale mean sea level pressure fields. The model accurately predicts fog and low-cloud days, illustrating the importance of large-scale pressure modulation and advective processes. It can be concluded that Namib-region fog is predominantly of advective nature, but also facilitated by increased radiative cooling. Seasonally different manifestations of synoptic-scale disturbances act to modify its day-to-day variability and the balance of mechanisms leading to its formation. The results are the basis for a new conceptual model on the synoptic-scale mechanisms that control fog and low clouds in the Namib Desert, and will guide future studies of coastal fog regimes.

1 Introduction

In moist climates, fog is typically viewed as an atmospheric phenomenon that disturbs traffic systems and negatively affects physical and psychological health (e.g., Bendix et al., 2011). In the hyperarid Namib Desert, however, the water input of

5 fog is key to the survival of many species (e.g., Seely et al., 1977; Seely, 1979; Ebner et al., 2011; Roth-Nebelsick et al., 2012; Warren-Rhodes et al., 2013; Henschel et al., 2018; Gottlieb et al., 2019). Despite this ecological significance, the local mechanisms that control the formation and spatiotemporal patterns of Namib-region fog are not yet fully understood, and potential linkages to synoptic-scale variability have yet to be explored. With regional climate simulations suggesting a warmer and even dryer climate (James and Washington, 2013; Maúre et al., 2018), fog could become an even more essential water

10 source for regional ecosystems in the future. However, the lack of understanding concerning fog and low-cloud (FLC) processes and their interactions with dynamics, thermodynamics, aerosols, and radiation in this region (Zuidema et al., 2016; Formenti et al., 2019) limits the accuracy of and confidence in projected changes of fog patterns (e.g., Haensler et al., 2011).

Field observations of local meteorological parameters and fog have led to the distinction between two main fog types occurring in the region: advection fog and high fog. Advection fog can form when a moist warm air mass is transported over

15 a cool ocean (Gultepe et al., 2007) and has been reported to occur mainly during austral winter, affecting a coastal strip of < 30–40 km (Seely and Henschel, 1998). High fog is described as a low stratus that frequently reaches more than 60 km inland between September and March and leads to fog where the advected stratus base intercepts the terrain (Seely and Henschel, 1998). While the two fog types are reported to be transported inland with different wind systems (for a review of local wind systems see Lindesay and Tyson (1990)), they are both described to be of advective nature. Recent analyses of diurnal FLC

20 characteristics have shown that the timing of FLC occurrence depends on the distance to the coastline, with FLCs occurring significantly earlier at the coast than further inland, which is an indication for the dominance of advective processes (Andersen and Cermak, 2018; Andersen et al., 2019). Also, measurements of fog microphysics during the AEROCLO-sA field campaign in the Namib suggest that the observed fog events were advected cloudy air masses from the ocean (Formenti et al., 2019). While it has long been acknowledged that other fog types (e.g., radiation fog and frontal fog) can occur in the Namib as

25 well (e.g., Jackson, 1941; Nagel, 1959), many statements regarding fog formation mechanisms in the historical literature do not seem to be founded on extensive and coherent observational evidence. Until recently, the occurrence of radiation fog, i.e. fog formation near the surface due to local radiative cooling under clear-sky conditions and without advective influence (Gultepe et al., 2007), was seen as a comparably rare situation (e.g., Seely and Henschel, 1998; Eckardt et al., 2013). This was questioned when, based on analyses of stable isotopes of fog water samples, Kaseke et al. (2017) and Kaseke et al. (2018) found

30 that the majority of their collected fog water samples stemmed from sweet water sources and interpreted this as evidence of predominant occurrence of radiation fog. Based on these findings, they postulated a potential shift from advection-dominated fog to radiation-dominated fog in the Namib Desert (Kaseke et al., 2017). Thus, the importance of the various fog formation mechanisms is currently a subject of scientific debate.

The goal of this study is to better understand the synoptic-scale conditions under which Namib-region FLCs occur, how synoptic-scale variability changes local conditions, and thereby to assess the relevance of different potential fog formation mechanisms. To this end, a 14-year time series of geostationary satellite observations of FLCs in the central Namib is combined with reanalysis data and air-mass backtrajectories to systematically analyze the large-scale dynamic conditions and air-mass characteristics that are associated with FLC occurrence in the Namib. The guiding hypothesis for this study is:

Fog and low clouds in the central Namib are primarily of advective nature and therefore associated with distinct synoptic-scale patterns of atmospheric dynamics and air-mass history. Thus, they can be statistically predicted with information on atmospheric circulation.

2 Data and methods

2.1 Satellite observations of FLCs

The Spinning-Enhanced Visible and Infrared Imager (SEVIRI) sensor, mounted on the geostationary Meteosat Second Generation (MSG) satellites, is ideally suited to provide spatiotemporally coherent observations of clouds. It features a spatial resolution of 3 km at nadir and scans its full disk every 15 min (96 hemispheric scans per day, (Schmetz et al., 2002)). In the context of this study, 14 years (2004–2017) of SEVIRI data in the thermal infrared are used to continuously detect FLCs with the algorithm developed by Andersen and Cermak (2018). In an extensive validation against surface observations, this technique has shown a good skill (97 % overall correctness of the classification). The 14-year FLC data set used here has already been applied to study spatial and temporal patterns of FLC occurrence along the southwestern African coast in Andersen et al. (2019). It should be noted that this satellite technique does not discriminate between fog and other low clouds.

The focus of this study is on FLCs in the central Namib, from where the majority of historical and present-day station measurements stem. To provide a representative measure of the overall central-Namib FLC cover on a daily basis, FLC occurrence is averaged between 3 UTC and 9 UTC (local time is UTC +2h) in the region between 22°S and 24°S and up to 100 km inland. Only pixels with at least a 5 % FLC occurrence frequency in the climatology (as in Andersen et al. (2019)) are used. The spatial and temporal averaging is illustrated for an exemplary day in Fig. 1 a). While the specific day shown here is arbitrary, the general feature of maximum FLC cover in the early morning hours and rapid decline shortly after sunrise is typical of the region (Andersen and Cermak, 2018). For further analyses, the data set is divided into 'FLC days' with mean regional FLC cover exceeding 50 % between 3 and 9 UTC, and 'clear days' with mean FLC cover below 3 %. These thresholds are chosen to represent two clearly separated parts of the FLC cover distribution that occur with similar frequencies. The resulting distribution of daily average FLC cover and the number of cases in each class are shown in Fig. 1 b). Figure 1 c) shows the monthly averages of central-Namib FLC cover, illustrating the general seasonal cycle of FLCs in this region.
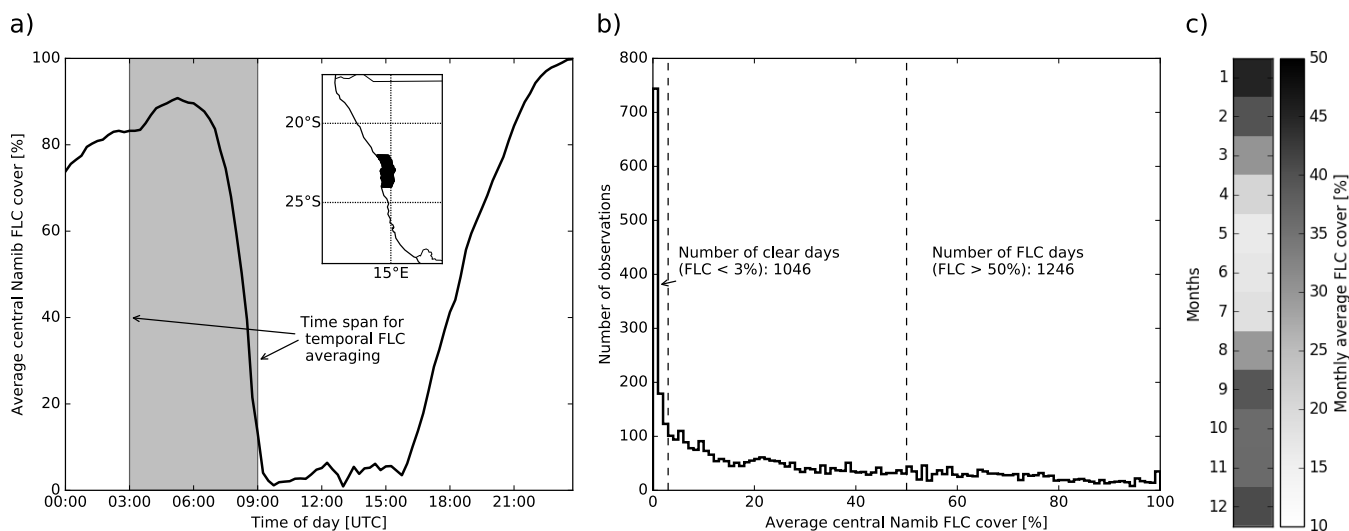
Figure 1. a) Illustration of the spatiotemporal averaging for one exemplary day (September 9th, 2015) to create the FLC cover data set. The curve in a) shows the regionally averaged (marked central-Namib region) FLC occurrence, which is then averaged between 3 UTC and 9 UTC (grey area). The resulting average daily morning FLC cover is given in percent. b) Distribution of the resulting central Namib FLC cover for the complete observation period (2004–2017). Observations are separated in two classes: clear days (<3 % mean FLC cover) and FLC days (mean FLC cover >50 %). Days with mean FLC cover between 3 % and 50 % are not considered in analyses based on this classification (2418 cases, for 404 days FLC cover could not be computed due to missing data or complete coverage with higher-level clouds). Panel c) shows monthly averages of the derived FLC cover data set.

2.2 ERA5 reanalysis

To investigate the large-scale meteorological conditions associated with FLCs in the central Namib, ERA5 reanalysis data from the European Centre for Medium-Range Weather Forecasts (ECMWF) are used. ERA5 is the new generation of reanalysis and follow-up of ERA-Interim (Dee et al., 2011). In comparison to ERA-Interim, it features higher spatial ($0.25°$) and temporal

5 (hourly) resolutions, along with other improvements (Hersbach, 2016).

In the context of this study, 14 years (2004–2017) of meteorological fields are analyzed. To characterize large-scale dynamic and thermodynamic conditions, fields of mean sea level pressure (MSLP), geopotential height at 500 hPa (Z500), u and v components of 10 m winds, 2 m air temperature (T2m), sea surface temperature (SST), total columnar water vapor (TCWV), specific humidity (Q), winds at different pressure levels, and lower tropospheric stability (LTS: computed as the difference

10 between potential temperature at 700 hPa and the surface, (Klein and Hartmann, 1993)) are used. To represent the morning conditions for which FLC is averaged, 6 UTC fields of ERA5 data are selected.

2.3 Trajectory analysis

24-hour backward trajectories are calculated using the Lagrangian Analysis Tool (LAGRANTO, (Sprenger and Wernli, 2015)). The three wind components needed for the trajectory calculations are taken from ERA5 on a regular 0.5° latitude-longitude grid, at 137 model levels in the vertical, and at a 3-hourly temporal resolution. The trajectories are started daily at 06 UTC for the period April, May, June, September, October and November 2004-2017. Their starting points are located in the central Namib close to Gobabeb at 23°S and 15°E 25 hPa above the surface, which corresponds roughly to 200 m above ground level. By doing so, the back trajectories represent air masses for the levels where fog and low clouds in the region are typically observed (Andersen et al., 2019). In order to obtain insights about the physical properties of the air masses, the temperature, potential temperature, specific humidity, and relative humidity are tracked along the trajectories. The location is chosen, as it is the main site of both historic and present-day scientific activity in the region (Lancaster et al., 1984; Seely and Henschel, 1998; Kaseke et al., 2017; Spirig et al., 2019).

2.4 Principal component analysis

The atmospheric variability of the South Atlantic and southern African region is characterized by means of a Principal Component Analysis (PCA). PCA solves the eigenvalues of the data covariance matrix and projects data variability onto an orthogonal basis, i.e. decomposes data variability into independent variability modes. Each mode explains a fraction of the total variance, and is represented by a spatial anomaly pattern and a standardized time series (namely, the principal components (PCs)) accounting for the amplitude of the anomaly pattern (cf. Storch and Zwiers, 1999). Here, the PCA is used to analyze daily fields of the zonal and meridional components of 10 m wind at 6 UTC in a domain centered on the Namib (0°–40°E; 40°S–0°N). The wind fields are first remapped onto a 2° regular grid, then daily 6 UTC anomalies are computed by subtracting the 14-year average wind components at each grid point. The PCA is applied to the covariance matrix of both components in the domain. In the context of this study, the main modes of the 10 m wind field variability are used to understand possible linkages between atmospheric dynamics and Namib-region FLCs.

2.5 Statistical prediction of FLCs

Statistical modeling of fog or low clouds is typically done by using local fields of a set of predictors, i.e. relevant meteorological fields and aerosol properties (e.g., Andersen et al., 2017; Adebiyi and Zuidema, 2018; Fuchs et al., 2018). The circulation-induced variability can be captured by spatial patterns of pressure fields (Deloncle et al., 2007; Yu and Kim, 2010; Sippel et al., 2019). A major challenge when using pressure fields (denoted $\mathbf{X}$, as an $n \times p$ matrix of n samples and p predictors located on a grid) to predict a target variable is, however, that the number of (strongly correlated) predictors can quickly outgrow the number of observations. This typically leads to high-variance problems (overfitting) in classical statistical models. The issue can be overcome with shrinkage methods, as e.g. regularized linear models (Hastie et al., 2001). These provide an extension of linear regression techniques that shrink the regression coefficients of a model by penalizing their size, thereby addressing the aforementioned high-variance issues (Hastie et al., 2001). Ridge regression is a specific example of a regularized linear model

where the shrinkage is controlled by a value λ that shrinks the coefficients of the model towards zero using the L2 penalty (the squared magnitude of the coefficient value is added as a penalty term to the loss function). This method is well suited for cases with a large number of correlated predictors that are all relevant (coefficients > 0) (Friedman et al., 2010). The method can be used for classification and regression (Friedman, 2012).

5   Here, the statistical learning method is used in a classification setting. That is, a binary response variable ("FLC day" or "clear day") is modeled using logistic regression regularized with the ridge penalty. In logistic regression with a binary response variable, the "odds ratio" ($log \frac{Pr(FLC\ day|X=x)}{Pr(clear\ day|X=x)}$) is estimated as a linear function of the predictors for any given day:

$$log \frac{Pr(FLC\ day|X=x)}{Pr(clear\ day|X=x)} = \beta_0 + \beta^T x, \qquad (1)$$

with β_0 the intercept and β^T the model coefficients. From the odds ratio, the estimated probabilities and the correspond-
10   ing class (FLC day or clear day) are determined for each sample. The ridge regression penalty based on the L2 norm, i.e. $R(\lambda) = \lambda \sum_{i=1}^{p} \beta_i^2$ is then incorporated as a constraint on the size of the regression coefficients in the objective function that is minimized to fit the model. The tuning parameter λ directly trades off between a more flexible regression model (small penalty, i.e., low λ value) but that possibly suffers from high-variance issues, and a less flexible regression model. Accordingly, a larger value of λ enforces smaller (but non-zero) regression coefficients, and a smoother spatial map of regression coefficients
15   is obtained as a result. The optimal λ value is derived through 10-fold cross validation. For a more complete description of regularized (logistic) regression, the reader is referred to Hastie et al. (2001), and the ElasticNet vignette for a hands-on tutorial (https://web.stanford.edu/~hastie/glmnet/glmnet_alpha.html). Model estimation and cross-validation was performed using the scikit-learn package in Python (Pedregosa et al., 2011).

The ridge regression method is used to predict FLC and clear days over the complete 14-year time series for which obser-
20   vations exist, using 6 UTC (representative of averaging time of FLC cover, see Sec. 2.1) ERA5 MSLP fields in a large spatial domain centered on the central Namib (0°S–45°S and 8°W–38°E, shown in Fig. 2). The ERA5 pressure fields feature a spatial resolution of $0.25° \times 0.25°$ and as such, lead to $33,485$ predictor fields.

3   Results and discussion

3.1   Dynamic and thermodynamic conditions

25   Figure 2 shows a climatology of the dynamic and thermodynamic characteristics of the southeastern Atlantic and southern African region based on 14 years (2004–2017) of ERA5 data. Two seasons are shown in the figure that are representative of two different fog regimes (described in the next paragraph, Seely and Henschel, 1998; Andersen et al., 2019): September, October, November (SON) in the left-hand panels and April, May, June (AMJ) in the right-hand panels. At this spatial scale, the St. Helena High and southern African continental high control the characteristic near-surface flow patterns during both
30   seasons. During SON, the St. Helena High is more prominent and, in combination with the thermal contrast between land and ocean, results in the formation of a low-level jet during this time (Nicholson, 2010). This coastal jet intensifies the upwelling

of cold water, which feeds back to amplify the jet by increasing the thermal land-ocean contrast (Nicholson, 2010). While more prominent during SON, the cold upwelling water of the Benguela current is apparent in the relatively low SSTs along the southwestern African coastline during both seasons (Fig. 2 c) and d)). During AMJ, continental high pressure situations are the most prominent circulation pattern (Tyson et al., 1996; Garstang et al., 1996). This is visible in the more pronounced southern

5 African continental high pressure system and leads to a marked amplification of the easterly flow over the southern African continent. In the Namib Desert, thermally and topographically induced local wind systems within the boundary layer modulate these synoptic air-flow patterns, and the significance of the induced diurnal oscillations can exceed that of the synoptic scale (Goldreich and Tyson, 1988; Lindesay and Tyson, 1990). The coastal marine regions adjacent to the Namib are characterized by stable conditions, specifically during SON (LTS contours in c) and d)). These stable conditions promote the formation of the

10 southeastern Atlantic stratocumulus cloud deck and determine its seasonal cycle (Klein and Hartmann, 1993; Andersen et al., 2017). One should note that MSLP and LTS are both affected by the high elevation of the central plateau in southern Africa and in this region (cf. Fig. 6), are not likely to be a perfect representation of near-surface pressure conditions and lower-tropospheric stability.

As outlined in the introduction, distinct seasonal FLC patterns have been identified in the central Namib (Lancaster et al.,

15 1984; Seely and Henschel, 1998; Cermak, 2012; Andersen et al., 2019). During SON, described as 'high FLC season' in Andersen et al. (2019), FLCs frequently occur in the central Namib as a low stratus or high fog (cloud base height on average ≈ 400 m above sea level (asl)) that touches the ground inland, whereas during the 'low FLC season' in AMJ, FLCs occur less frequently, do not extend as far inland and are typically lower, at ≈ 200 m asl and thus register as fog (termed 'advection fog' in Seely and Henschel (1998)) at locations closer to the coastline (Andersen et al., 2019). It has been assumed that the

20 occurrence of Namib-region FLCs and their variability on diurnal to seasonal scales is driven by the position and strength of large-scale pressure systems, as this would affect formation and advection of low-level clouds, atmospheric stability (Lancaster et al., 1984; Cermak, 2012; Andersen and Cermak, 2018; Andersen et al., 2019), as well as SST patterns (cooling of air masses) and the presence and position of a coastal low that has been linked to fog occurrence (Olivier and Stockton, 1989). While all of these links are plausible and likely play a role for FLCs in the Namib, a more in-depth analysis is needed to estimate the

25 importance of the different mechanisms.

3.2 Differences in meteorological conditions on FLC days and clear days

Figure 3 shows large-scale patterns of averaged monthly mean differences in a) MSLP and 10 m winds, b) Z500 and winds at the same pressure level, c) T2m, d) LTS, e) SST, and f) TCWV on FLC versus clear days (as defined in Sec. 2.1) in the central Namib (marked with a star) during the investigated 14-year period (all months are considered here). The average of monthly

30 mean differences is chosen rather than the overall mean differences to account for the distinct seasonal cycle of FLC occurrence in the Namib (Fig. 1 c)). In each pixel, an independent two-sided t-test is computed to identify significant differences between the two classes (contours show p values <0.01). It is apparent that the dynamical conditions (Fig. 3 a) and b)) on FLC days differ significantly on the synoptic scale. On FLC days, MSLP over continental southern Africa is systematically lower by about 3–5 hPa. This anomaly of lower MSLP extends over the southeastern Atlantic ocean at about 30°S. In a smaller oceanic
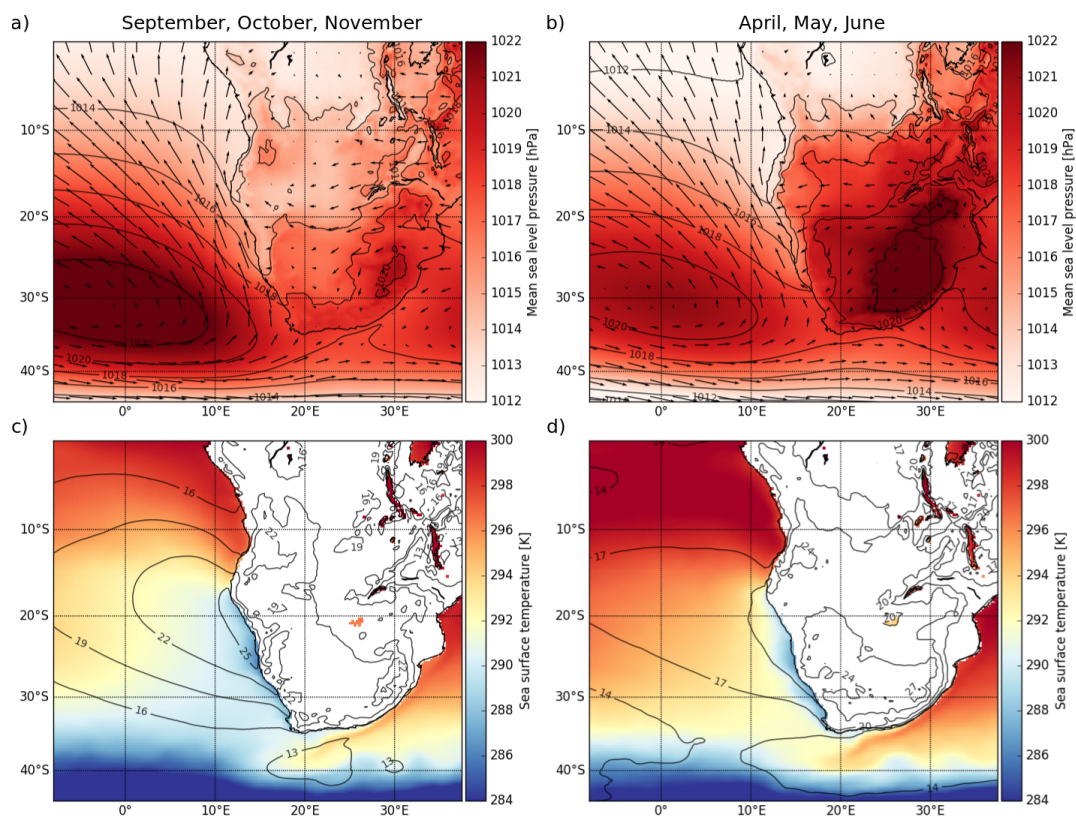
Figure 2. Climatological setting of the region in two seasons (2004–2017): September, October, November on the left and April, May, June on the right. Top row: MSLP in color and contours with 10 m winds indicated by arrows where the length scales with strength (the u and v vectors of near-surface winds are bilinearly interpolated to a $2.5° \times 2.5°$ grid for clarity). Bottom row: SST in color, LTS (K) as contours. Data is sampled at 6 UTC.

region along the coastline north of 23°S, MSLP is significantly higher, leading to an overall anomalously high land-sea pressure gradient in this region and an onshore flow anomaly of near-surface winds in the central Namib on FLC days. The land-sea contrast in MSLP indicates a heat low over land, where the heat anomaly (Fig. 3 c)) could be driven by northerly advection ahead of the trough or enhanced surface warming. Z500 on FLC days is significantly lower over the southeastern Atlantic

5   between 30°S and 40°S. This pattern is an indication for upper-level waves disturbing the mean tropospheric circulation of the southeastern Atlantic and southern Africa (Tyson et al., 1996; Fuchs et al., 2017). In combination, MSLP and Z500 show a weakly baroclinic structure with the mid-level trough shifted to the west. There is, however, no indication of the predominant presence of a coastal low that has been described in Olivier and Stockton (1989) as a local feature that can determine onshore flow. The presence of such a coastal low, at least in some of the cases, may be masked by the stronger pressure anomalies of

10 the synoptic scale.

There is a coherent pattern of slightly lower SSTs (≈ 0.5 K: Fig. 3 e)) along the coastline on FLC days; however, the difference between SSTs on FLC and clear days is not significant at the 0.05 level. It is interesting to note that SSTs tend to be lower on FLC days, although the coast-parallel near-surface wind that partly governs the upwelling is slightly weaker in these cases (Fig. 3 a)), potentially hinting at a time-lag response of SSTs. The observed low anomaly of SSTs close to
5 the coast at $\approx 15°$S may also have a hydrostatic (positive) impact on MSLP in that region. It appears likely that effects of SST patterns on FLC variability are most pronounced on seasonal to inter-annual scales as observed in the Chilean Atacama desert (Del Río et al., 2018). Differences in TCWV on FLC and clear days are pronounced (Fig. 3 f)). A coherent region of a significantly dryer column stretches from the central Namib over the coastal Atlantic, where the anomaly is strongest. This is likely the dry slot (Browning, 1997) or dry air intrusion of the synoptic-scale disturbance that leads to increased longwave
10 cooling and can thereby facilitate the formation of FLCs. A substantial moist anomaly is visible over the southern African continent, likely driven by large-scale free-tropospheric moisture transport from the north west (Fig. 3 b)). These moist air masses may contribute to the observed T2m heat anomaly via greenhouse warming (Fig. 3 c)). Along the coastal strip that is typically overcast with FLCs (Olivier, 1995; Cermak, 2012; Andersen and Cermak, 2018; Andersen et al., 2019), T2m is significantly lower by about 4 K, which is likely a feedback of FLCs slowing down the surface heating in the early morning,
15 or due to air-mass differences. The observed difference patterns in LTS (Fig. 3 d)) between FLC and clear days matches those of T2m so that they can be assumed to be mostly driven by its surface component.

The observed anomaly patterns indicate that different mechanisms are triggered by the observed synoptic-scale disturbances and may contribute to FLC occurrence in the central Namib in two main ways:

1. Enhanced formation of FLCs due to increased longwave cooling under the dry anomaly close to the coast.

20 2. Onshore flow anomaly of marine boundary layer air masses due to a) a modulation of coastal winds and b) a formation of a southern African heat low due to greenhouse warming by moist air masses and northerly warm air advection.

As both synoptic and FLC characteristics differ substantially between the SON and AMJ, the following section focuses on specific characteristics and differences of these mechanisms during these seasons.

3.3 Seasonal differences in synoptic-scale mechanisms

25 Figures 4 and 5 show seasonally averaged differences between FLC and clear days of all analyzed parameters during the two seasons SON and AMJ. During both seasons, MSLP (Fig. 4 a) and b)) and Z500 (Fig. 4 c) and d)) indicate synoptic-scale disturbances on FLC days. However, seasonal differences exist, as during SON, these anomaly patterns suggest a cut-off low, while the marked bipolar pattern of the anomalies in AMJ suggests the presence of a breaking Rossby wave. The negative continental MSLP anomalies on FLC days are larger during AMJ, likely amplified by the more pronounced T2m anomalies
30 and subsequent effects on a continental heat low during this time (cf. Fig. 5 c) and d)). As noted above, the continental heat anomaly can be caused by northerly warm air advection or enhanced warming due to changes in the radiative balance. The observed seasonal MSLP and 10 m wind anomalies (Fig. 4 a) and b)) that result in a transport of warm air from the northeast into the anomaly region (not shown), as well as the TCWV anomalies (Fig. 5 a) and b)) suggest that during SON, the heat
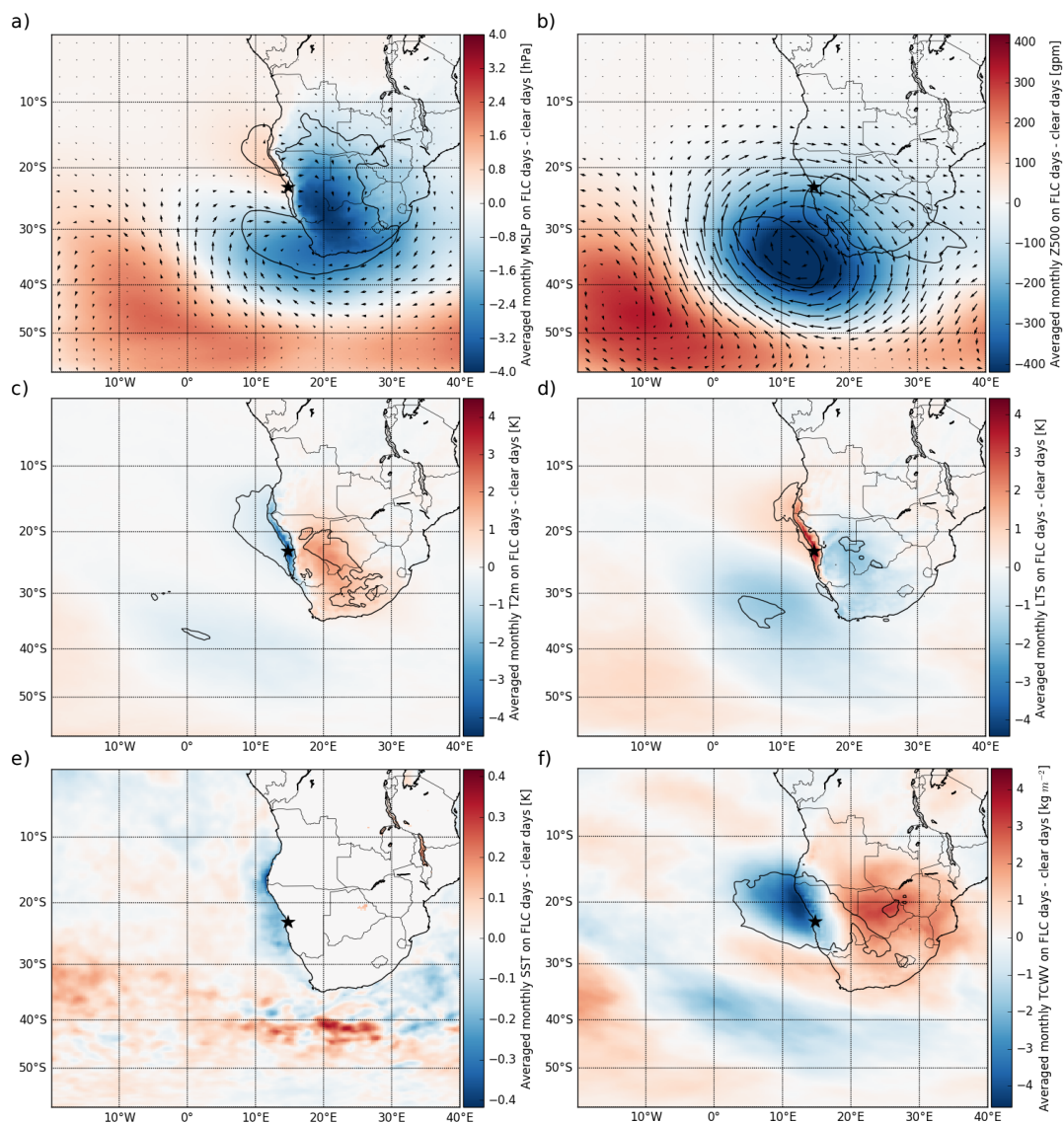
Figure 3. Averaged monthly mean differences (FLC days - clear days) of a) MSLP and 10 m winds, b) Z500 and 500 hPa winds, c) T2m, d) LTS, e) SST, and f) TCWV at 6 UTC. In each pixel, an independent two-sided t-test is computed to identify significant differences between FLC and clear days for each month. Contours mark regions where the distributions differ significantly at the 0.01 level (median of the monthly p values < 0.01). U and v vectors of winds are interpolated as in Fig. 2.

anomaly on FLC days is mostly due to northerly advection of warm air, whereas during AMJ, TCWV is significantly increased over the southern African continent, especially in regions of high T2m anomalies. Here, the increased moisture causes an additional surface heating due to greenhouse warming. It is likely that the TCWV anomaly is caused by a large-scale free-tropospheric moisture transport from the tropics, which is supported by the marked wind anomalies at 500hPa (Fig. 4 d)) that

show a northwesterly anomaly. It should be noted that a Lagrangian transport of moisture at this scale takes time and as such is likely to occur when the Rossby wave disturbance is relatively stationary or if two consecutive systems pass within a short timeframe (Knippertz and Martin, 2005).

A few 100 km to the west and south of the Namibian coastline, SSTs (cf. Fig. 4 f)) are significantly higher on FLC days during AMJ, potentially leading to increased moisture within the marine boundary layer. It is not clear yet, however, what drives the observed anomaly pattern of SSTs during AMJ. While the seasonally varying TCWV and SST anomalies illustrate the seasonal variability in the mechanisms that can contribute to FLC occurrence in the central Namib, during all months, the outlined systematic patterns of significant negative MSLP anomalies over continental southern Africa and the localized coastal high pressure anomaly are apparent. It can be concluded that a low pressure anomaly in continental southern Africa and the associated onshore advection of marine boundary layer air masses facilitates FLC occurrence in the central Namib during the entire year.

To better understand the characteristics of the observed moisture transport and its relevance for central-Namib FLC occurrence, information on the vertical patterns of moisture and wind anomalies is needed. Figure 6 shows average seasonal differences of Q and winds on FLC versus clear days at different pressure levels during a) SON and b) AMJ (averaged between 20°S and 25°S). During both seasons, a complex vertical structure of Q anomalies is apparent that is assumed to be disturbance-induced. During both seasons, the marine boundary layer features an onshore flow anomaly and is more humid on FLC than on clear days, especially during AMJ. These differences are caused by the subsiding dry continental easterly air masses that dominate on clear days, whereas on FLC days, a slight onshore flow of the more humid marine boundary layer air is observed in the central Namib. Over land, these marine air masses flow against the dominant continental easterly winds (Lindesay and Tyson, 1990), producing a northerly wind flow at $\approx 15°N$ (not shown) that has been found to be associated with fog occurrence in the central Namib (Seely and Henschel, 1998; Spirig et al., 2019). Above the moist marine boundary layer, the free troposphere is relatively dry on FLC days during both seasons, a feature which is not visible in the columnar TCWV composites during AMJ as it is masked by the moist anomaly in the marine boundary layer (Fig. 5 a)). The seasonal difference in the free-tropospheric Q anomalies over the continent is clear and the vertical distribution of Q anomalies during AMJ corroborates the assumption that the observed positive TCWV anomalies are due to free-tropospheric moisture transport (Fig. 5 b)). Expressed in relative terms, Q is about halved within the dry anomaly region on FLC days during both seasons, suggesting that radiative cooling is an important factor for FLC formation, especially over marine regions where the dry anomaly is most pronounced. During AMJ, the free-tropospheric relative moisture difference between FLC days and clear days is observed to be as high as 220 %. This substantial increase in free-tropospheric moisture in this otherwise dry central plateau region induces a substantial surface heating, contributing to the formation of the observed heat low, which modulates regional wind systems and leads to the onshore flow anomaly.

3.4 The role of air-mass history and dynamical regimes

Air-mass backtrajectories, initiated in the central Namib close to Gobabeb at 23°S and 15°E (indicated by the star in Fig. 7), 6 UTC and 25 hPa above ground level (approximates 200 m above ground level), are computed for the 14-year observational
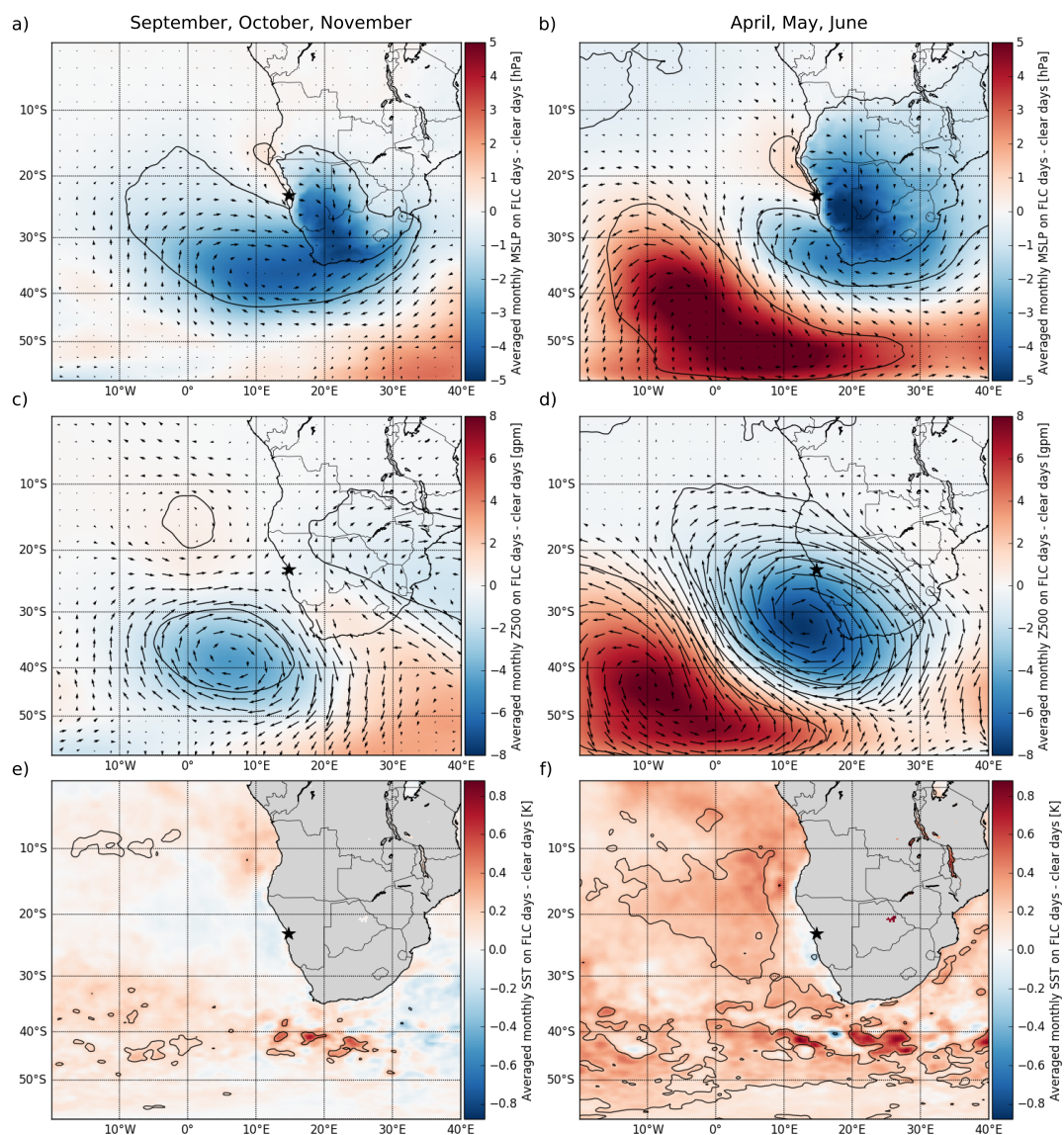
Figure 4. Mean of monthly average differences (FLC days - clear days) during SON (left-hand panels) and AMJ (right-hand panels) of MSLP (top), Z500 (middle), and SST (bottom) for the time period 2004–2017. Contours mark significant differences as in Fig. 3. Wind anomalies at 10 m (top) and 500 hPa (middle) are superimposed as vectors.

period. Figure 7 shows the backtrajectories for FLC days (top) and clear days (bottom) for the two seasons SON (left-hand panels) and AMJ (right-hand panels). During both seasons, air masses on FLC days nearly exclusively stem from the marine boundary layer and have traversed over the cool upwelling ocean water along the coastline for the time span of 24 h. While the number of FLC days during SON is higher than during AMJ, following the general seasonality of FLCs in the region

5   (cf. Fig. 1 c)), no clear seasonal differences in air-mass dynamics can be observed in such situations. This suggests that during
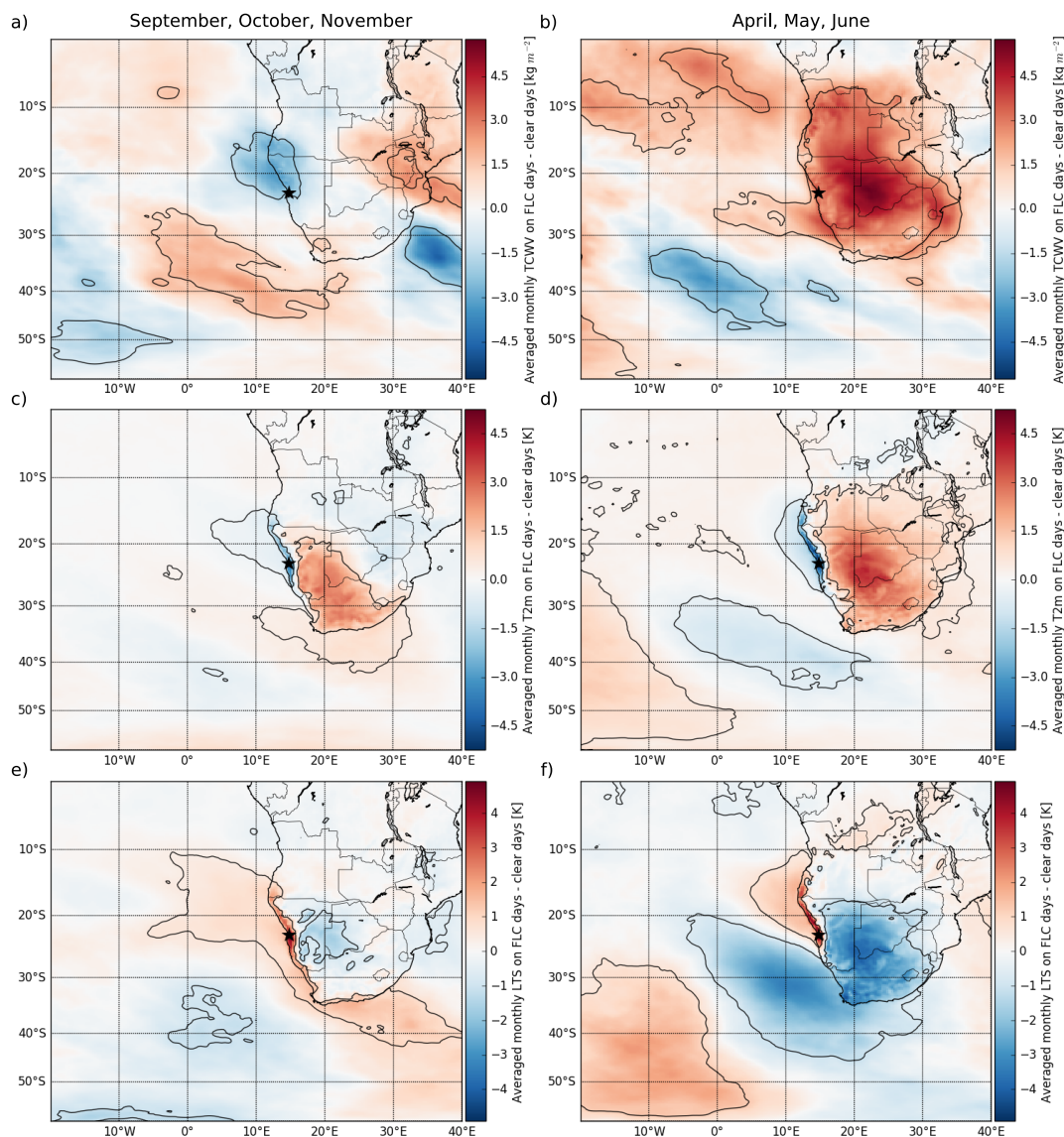
Figure 5. Mean of monthly average differences (FLC days - clear days) during SON (left-hand panels) and AMJ (right-hand panels) of TCWV (top), T2m (middle), and LTS (bottom) for the time period 2004–2017. Contours mark significant differences as in Fig. 3.

both seasons, similar local dynamic conditions drive FLCs or air masses that develop into FLCs inland into the Namib desert, but that due to seasonal differences of large-scale dynamics, these situations occur with varying frequency during different seasons.

On clear days, air-mass histories are more diverse and show distinct seasonal differences, but are frequently characterized by subsiding continental air masses. While on clear days during SON, a considerable fraction of the air masses is still transported
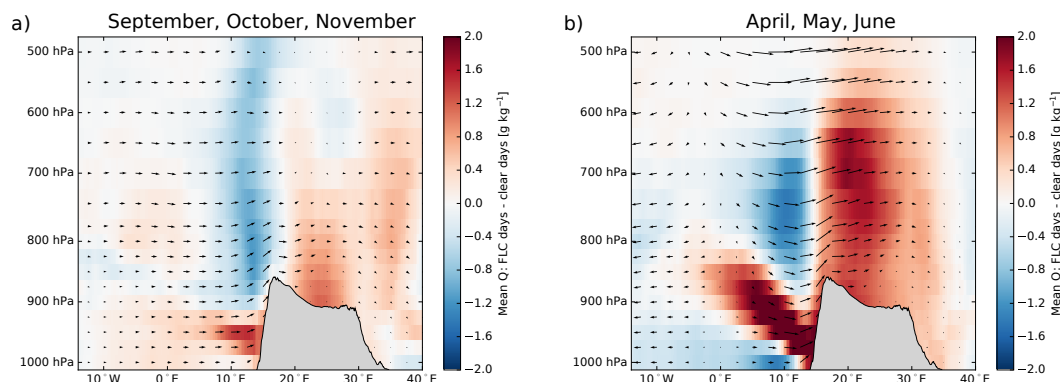
Figure 6. Seasonal average difference (FLC days - clear days) in specific humidity, and u and w wind components at different pressure levels during a) SON and b) AMJ for the time period 2004–2017. Specific humidity and wind vectors are averaged between $20°$S and $25°$S and shown at pressure levels between 1000 hPa and 500 hPa. For illustration purposes, the w vector is enhanced by a factor of 20. The masked grey area approximates the average surface elevation between $20°$S and $25°$S.

from the marine boundary layer, during AMJ, subsiding north-easterly continental air masses dominate. This seasonal shift in air-mass dynamics is likely driven by the seasonality of the two dominating high pressure systems of the region that is shown in Fig. 2. During AMJ, the southern African continental high pressure system is enhanced and leads to the stronger easterly flow. These observations support the hypothesis by Lancaster et al. (1984) that the seasonality of fog in the central Namib is to some

5   extent controlled by the Southern African high pressure system, as the associated easterly winds are likely to inhibit large-scale onshore advection of cloudy marine boundary layer air masses. The results also suggest that aerosols from the biomass burning season in continental southern Africa (Swap et al., 2003) are unlikely to play a large role for fog formation by acting as cloud condensation nuclei, as biomass burning aerosols within the boundary layer are mostly associated with continental air masses in this region (Formenti et al., 2018). However, biomass burning aerosols may influence Namib-region FLCs by absorbing

10   solar radiation and modifying the thermodynamic conditions, which has been observed and modeled to influence the Namibian stratocumulus deck (Zhou and Penner, 2017; Deaconu et al., 2019).

While systematic differences in air masses exist between FLC days and clear days, clear days may still feature air masses that are advected from the marine boundary layer (cf. Fig.7 c)). To understand the differences between the FLC days and clear days in such situations, these are isolated and analyzed in the following. Figure 8 shows the average Q, relative humidity

15   (RH), air temperature (T), and pressure (P) along all those backtrajectories that are advected from the marine boundary layer (here: P > 900 hPa over ocean). It is apparent that these air masses contain significantly more moisture on FLC days than on clear days, which explains most of the difference in RH. The backtrajectories of FLC days feature a stronger cooling during the last 10 hours of advection (hours 0–10), resulting in an additional increase in RH. The deviation in T between FLC and clear days seems to be driven by the vertical movement of the air masses. Ten hours before initialization, air masses

20   on clear days are located ≈20 hPa higher than on FLC days, not cooling off as they are advected due to their simultaneous subsidence. Other potential factors that may drive the observed deviation in T, such as the free tropospheric moisture content
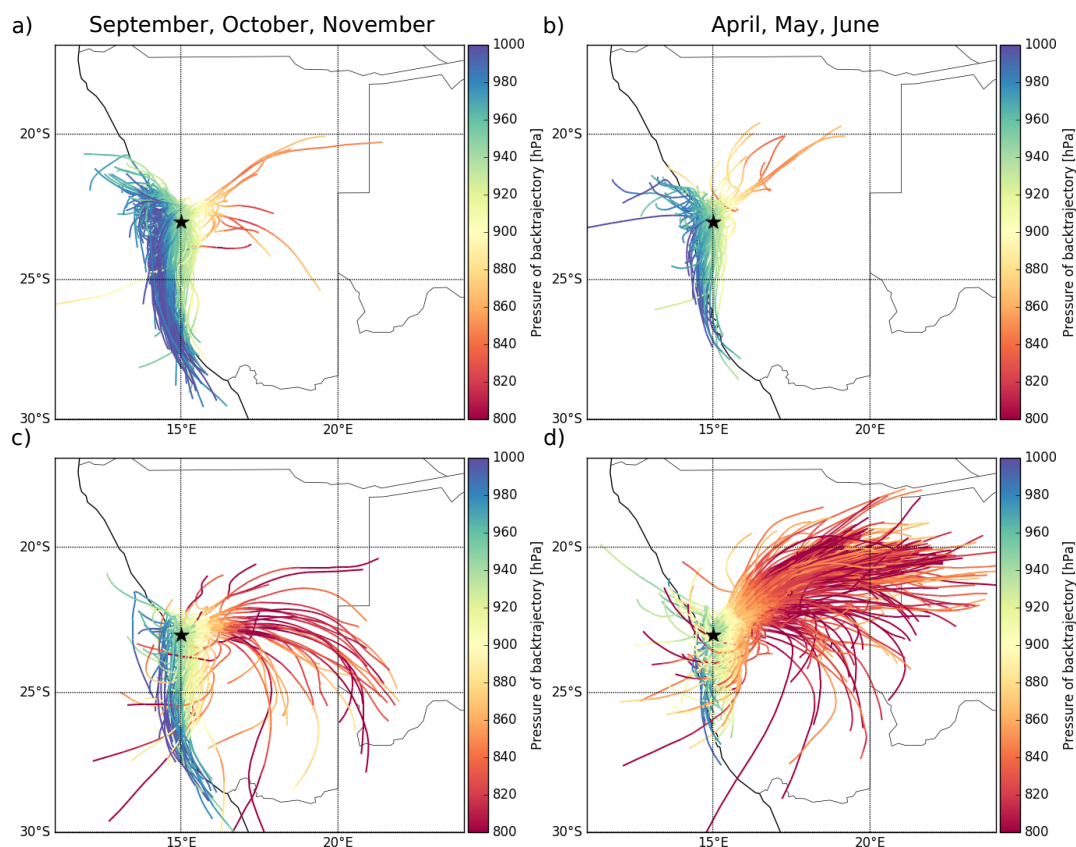
Figure 7. 24-hour Lagranto air-mass backtrajectories for FLC days (top) and clear days (bottom) in September, October, November (left-hand panels) and April, May, June (right-hand panels) for 2004–2017. The star marks 23°S and 15°E, where the backtrajectories were initialized at 25 hPa (approximates 200 m) above ground level. The number of samples are a) 363, b) 133, c) 135 and d) 452. For technical reasons, ≈10 % of the trajectories in panels a) and c) could not yet be calculated, but due to the clarity of the observed patterns that are already based on a high number of trajectories, this is not thought to influence the general results in a meaningful way.

and the surface temperature along the backtrajectories, were not found to be systematically different on FLC and clear days (not shown). These findings highlight that Namib-region FLCs are not only dependent on dynamics, but that marine boundary-layer moisture content as well as temperature changes during advection are important controls as well.

It is likely that the computed air-mass backtrajectories do not fully capture thermally and topographically induced local air flow patterns (see Lindesay and Tyson (1990) for a review) that contribute to local FLC occurrence patterns and possibly formation. However, the larger-scale patterns of air-mass history of marine boundary-layer air masses versus the subsiding continental air masses from the free troposphere are clearly evident from the analysis presented and offer a consistent physical explanation of the large-scale FLC occurrence patterns. The observations suggest that Namib-region FLCs are either advected after forming over the cool adjacent ocean or that condensation takes place during advection of the marine boundary-layer air
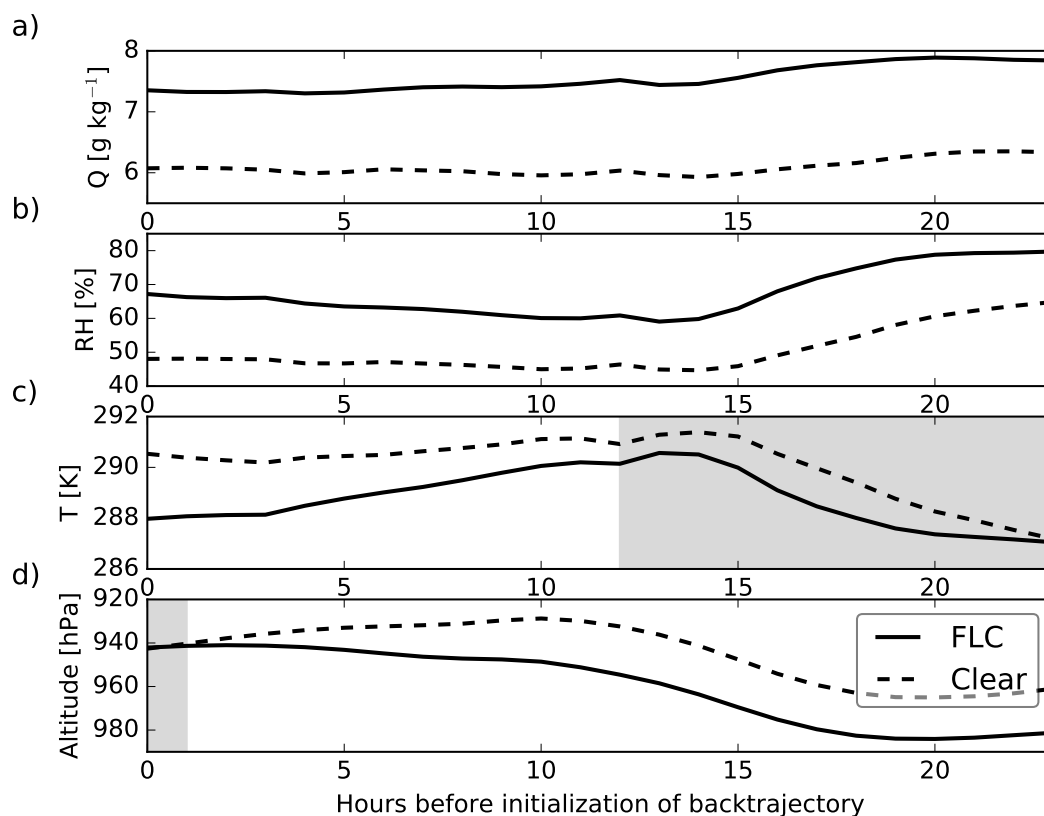
Figure 8. Hourly averaged specific humidity (a)), relative humidity (RH, b)), temperature (T, c)), and pressure (P, d)) along the 24-hour air-mass backtrajectories that are advected from the marine boundary layer on FLC days and clear days during SON 2004–2017. The number of samples are 333 FLC days and 74 clear days. Grey shading highlights non-significant differences.

masses over land due to higher humidity levels, lower temperatures or radiative cooling, though a mix of these processes is likely.

A PCA is conducted on spatial patterns of synoptic-scale near-surface winds (see Sec. 2.4 for details on the method) to analyze to what extent Namib-region FLCs are connected to specific dynamical regimes. Figure 9 a) shows correlations between daily central-Namib FLC cover and the PCs associated with the first six modes of variability of near-surface winds during all months of the year. All PCs are significantly correlated to FLC cover during some months of the year. Clear correlation patterns are evident: PCs 1, 4 and 5 show negative correlations with FLC cover, while PCs 2, 3 and 6 feature positive correlations. These PCs that facilitate FLC occurrence (2, 3, 6) all show westerly or northwesterly wind anomalies in the central Namib, while PCs that are negatively associated with Namib-region FLC cover feature anomalously strong continental easterly winds, consistent with results presented in Sec. 3.2 and 3.3. Panels c) and d) of Fig. 9 show the spatial patterns of near-surface wind anomalies of PCs 3 (explained variance: 11 %) and 4 (explained variance: 6 %), as examples for PCs that promote and impede FLC

occurrence, respectively. A seasonal dependence of the correlations between PCs and FLC cover is apparent and seems to
be related to the seasonality of FLC cover (Fig. 9 b)): PCs associated with onshore circulation in the central Namib feature
the strongest positive correlations during winter when FLC cover is generally lowest over the Namib, especially evident for
PC 3. This appears plausible, as during winter, the typical dynamical setting is less conducive to FLCs (see Fig. 2 for fall/early
5   winter conditions during AMJ), and consequently, FLC occurrence is dependent on a stronger dynamical disruption during this
time. During summer, when FLCs frequently occur in the central Namib, dynamical conditions associated with PCs 4 and 5
(dominance of continental easterlies) seem to impede the occurrence of FLCs. The results underscore that the advection of
marine air masses is crucial for the occurrence of FLCs in the central Namib.
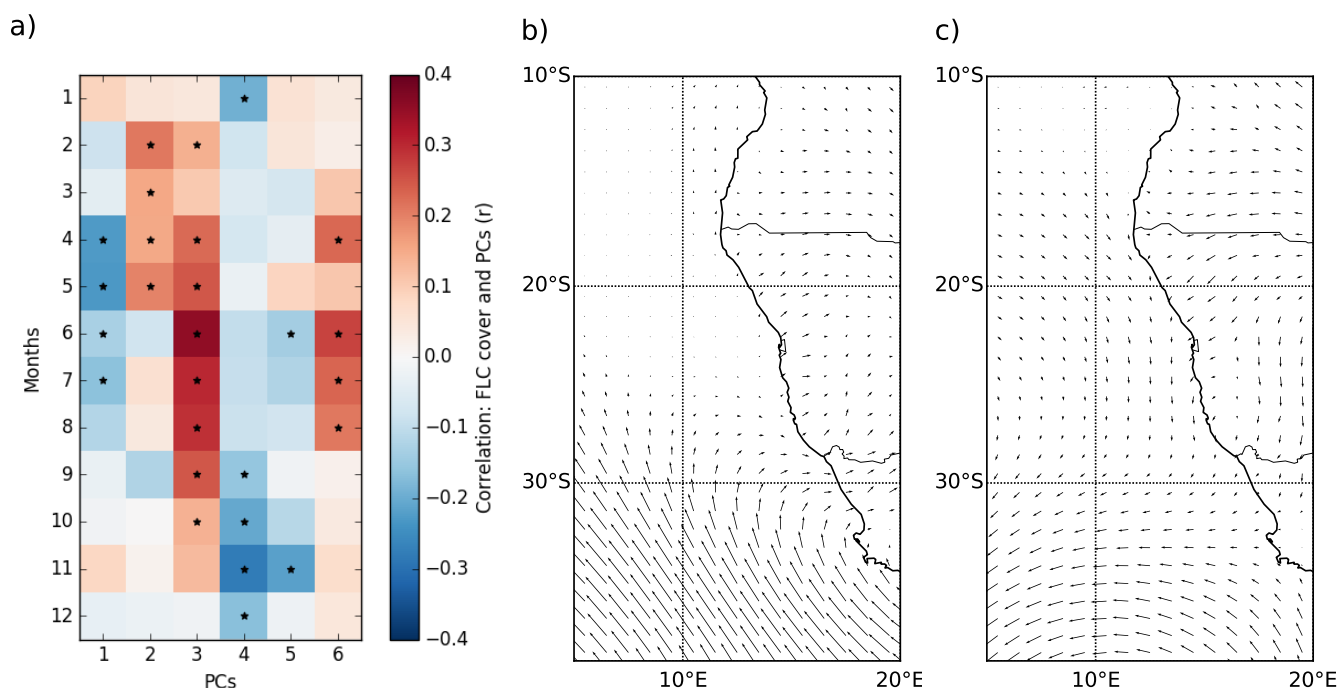
Figure 9. a) Correlations (Pearson r) between the PCs (associated with the empirical orthogonal functions of the spatial wind patterns) and
central-Namib FLC cover. Stars mark correlations that are significant at the 0.01 level. Panels b) and c) show wind anomaly fields for PCs 3
and 4, respectively. For visual clarity, spatial wind anomalies are shown for regional cutouts of the spatial domain that is considered in the
PCA and averaged to a $1° \times 1°$ resolution (see Sec. 2.4 for details on the analysis).

3.5 Statistical fog and low-cloud prediction with pressure fields

10   Based on the evidence presented above, showing that FLC occurrence is tightly connected to synoptic-scale patterns, it can be
assumed that FLC occurrence can be predicted to some extent with a statistical learning technique that utilizes spatial patterns
of dynamical information. Here, a ridge regression is applied to classify FLC days and clear days based on MSLP fields in a
region spanning $45° \times 45°$ that is centered on the central Namib (see Sec. 2.4). MSLP fields are used, as their anomaly patterns

on FLC days are similar during the different analyzed seasons and thus summarize the controlling mechanisms of onshore advection of marine boundary-layer air masses. Figure 10 a) shows the resulting coefficients, i.e. regression slopes, of the statistical model. The sign and spatial patterns of the coefficients are similar to the observed MSLP anomalies shown in Fig. 4, where coefficients (and anomalies) are negative in the inland region of Namibia, and positive and along the northern part of the

5 Namibian coastline. It should be noted that the statistical model seems to mostly rely on regional MSLP fields, resulting in low coefficients at the synoptic scale, e.g., the Atlantic high pressure system. It can be concluded that the synoptic-scale pressure patterns set the stage for more localized pressure and wind modulations that determine FLC occurrence, and that regional MSLP fields contain information on both.

Figure 10 b) gives a summary of statistical measures of the skill of the model to classify between FLC and clear days in

10 the central Namib. Using MSLP fields at 6 UTC on the day of the FLC cover information, the ridge regression model has a probability to correctly detect FLC days of 94 % with 17 % of the reported FLC days being false alarms, leading to an overall correctness of the model of 86 % and a positive bias of 14 %. The critical success index (CSI: 0.79), and the Heidke skill score (HSS: 0.72) combine these scores and show that the model is skillful in distinguishing between the defined fog and clear days. The colored dots in Fig. 10 b) illustrate the progression of the model skill when the training is carried out based on MSLP fields

15 of one, two, three or four days prior to the FLC observation. While, as expected, the model skill deteriorates with an increasing temporal gap between the MSLP predictors and the time of FLC occurrence, the model is capable of predicting fog occurrence fairly well one day in advance, as the time series of day-to-day FLC occurrence features a significant autocorrelation. To some extent, this may be connected to the strong persistence of synoptic-scale dynamics in the subtropics. Even though the model only uses MSLP fields, ignoring e.g. effects of radiative cooling due to moisture anomalies, surface temperatures, and seasonal

20 characteristics, which have been shown to modify FLC occurrence, the results still illustrate the potential of a dynamics-based statistical fog forecast in this region.

It should be noted that the distinction between fog and clear days is based on spatially and temporally averaged FLC occurrence (see Sec. 2.1) and that days are omitted that feature an FLC cover between 3 % and 50 %. Also, the exact location and time of FLC occurrence is likely to be dependent on local temperature gradients and topography that lead to local modulation

25 of winds (Lindesay and Tyson, 1990). Still, the model produces promising results that may be built upon in future studies by testing a similar model setup to predict the timing and duration of FLCs at specific locations.

4   Summary and conclusions

In this study, the occurrence of FLCs in the Namib desert, derived from 14 years of satellite observations, is systematically analyzed within the context of the regional climate and related to large-scale patterns of MSLP, Z500, T2m, LTS, SST, TCWV

30 as well as Q and winds at different pressure levels from ERA5 reanalyses. The satellite data set of FLC occurrence is separated into FLC days and clear days that are further investigated in terms of their meteorological conditions, air-mass histories and statistical predictability during two seasons (AMJ and SON).
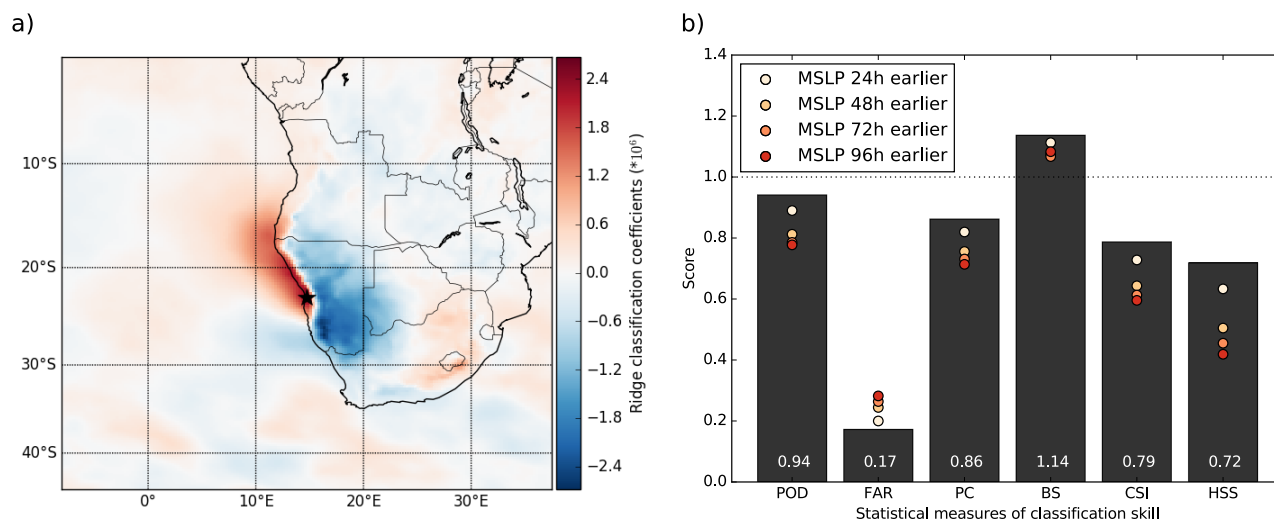
Figure 10. a) The coefficients of the ridge regression used for classification of FLC days versus clear days. b) Statistical measures of the performance of the ridge regression to classify FLC days versus clear days. The bars and related numbers describe the model skill using 6 UTC MSLP fields of the day of FLC observation and relate to a). The colored dots show the model skill when the model is trained on MSLP fields of one to four days earlier. The abbreviations of the statistical measures stand for probability of detection (POD), false alarm rate (FAR), percent correct (PC), bias score (BS), critical success index (CSI), and the Heidke skill score (HSS). The equations of the statistical measures are given in the appendix.

It is found that MSLP and Z500 patterns on FLC days are systematically and significantly different from clear days on synoptic scales. On FLC days, a systematic pattern of significantly lower MSLP over continental southern Africa is observed, which, in combination with higher pressure over a marine coastal region at about 20°S, leads to an onshore flow anomaly of marine boundary-layer air. Together with significantly lower Z500 in the southeastern Atlantic region on FLC days, these dynamic patterns are an indication for a cut-off low during SON and a breaking Rossby wave during AMJ. As cut-off lows are

5 typically associated with Rossby wave breaking events in the southern hemisphere (Ndarana and Waugh, 2010), these synoptic-scale disturbances may be viewed as different stages of similar systems. Both modify circulation systems, which in turn alter moisture transport, resulting in characteristic moisture patterns on FLC and clear days. Over the coastal boundary layer, the free troposphere is observed to be significantly drier on FLC days during both seasons, increasing radiative cooling, which

10 likely contributes to FLC formation, especially over the ocean where the dry anomaly is observed to be most pronounced. During AMJ, free-tropospheric moisture over the southern African continent is substantially increased, leading to greenhouse warming at the surface. While northerly warm air advection also contributes to the observed positive T2m anomalies on FLC days (during both seasons), the additional increase in T2m on FLC days during AMJ clearly corresponds to regions of increased free-tropospheric moisture content. The increase in T2m leads to the development of a heat low that amplifies the upper-level

15 disturbance-induced low MSLP anomaly, thereby contributing to the onshore flow anomaly of marine boundary-layer air masses. In the localized coastal region where FLCs typically occur, T2m is found to be significantly lower on FLC days, likely

a combination of a local feedback of FLCs that slow down surface heating in the morning hours, and air mass differences. A significant pattern of SST anomalies is found only in AMJ, with anomalously high SSTs off the coast that may contribute to higher marine boundary-layer humidity.

The analysis of backtrajectories initialized in the central Namib at typical cloud level shows systematic differences in air-mass dynamics on FLC days and clear days. Air masses on FLC days are nearly exclusively transported within the marine boundary layer over the cool upwelling waters along the coastline, whereas clear days are frequently associated with subsiding northeasterly air masses, especially during AMJ. During SON, when advection of marine-boundary layer air masses can also occur on clear days, air masses on clear days feature significantly less moisture and tend to be advected from higher altitudes than on FLC days. The findings clearly demonstrate the strong dependence of central-Namib FLC occurrence on the advection of moist marine boundary-layer air masses, contrasting the notion of predominant radiation fog (Kaseke et al., 2017), but in agreement with many other studies (e.g. Seely and Henschel, 1998; Formenti et al., 2018; Andersen et al., 2019; Spirig et al., 2019). These results are supported by a principal component analysis of near-surface winds that show a clear connection of FLC cover to synoptic-scale dynamics. Principal components of spatial wind patterns that feature positive onshore flow anomalies are positively related to FLC cover. This relationship is especially strong during winter, when FLC occurrence is at its minimum, as then, the dominant continental easterly flow typically inhibits inland advection of FLCs or locally developing FLCs. This suggests that during this time, a stronger dynamical forcing is needed to overcome this characteristic flow that is unfavorable for inland advection of cloudy marine boundary layer air masses.

As the results show that spatial pressure patterns are connected to FLC occurrence, a ridge regression model is used to classify FLC days versus clear days based on regional MSLP fields. The resulting spatial pattern of model coefficients is similar to the observed MSLP anomaly patterns within the region of Namibia and the adjacent ocean areas. The spatial domain of relevant model coefficients seems to be smaller than the spatial extent of the pressure anomalies, probably because the regional fields contain information on synoptic-scale disturbance as well as local modulation. On this basis, the model is capable of skillfully delineating FLC days from clear days. The model is trained with MSLP fields with different temporal offsets, and found to be capable of skillfully predicting FLC occurrence one day in advance, highlighting the potential of a statistical forecast of FLCs in this region. Future work should focus, however, on the development of a statistical model that links information on e.g. MSLP, free-tropospheric moisture, SSTs, Z500 and aerosol loading with FLC occurrence to quantify the effects of the different processes and mechanisms outlined in this study.

The findings of this study suggest that FLCs in the central Namib are facilitated by synoptic-scale disturbances in two main ways:

1. Increased longwave cooling due to an anomalously dry free troposphere, especially over the ocean that facilitates the formation of low clouds.

2. Onshore flow anomaly of these cloudy marine boundary layer air masses due to

   a) disturbance-induced modulation of local winds, and

   b) a heat low over continental southern Africa.

The magnitude and characteristics of the disturbance and the related mechanisms depend on season, with a more pronounced disturbance during AMJ, when the typical dynamic setting is less conducive to FLC occurrence. Figure 11 is a schematic illustration that summarizes these seasonally varying mechanisms.
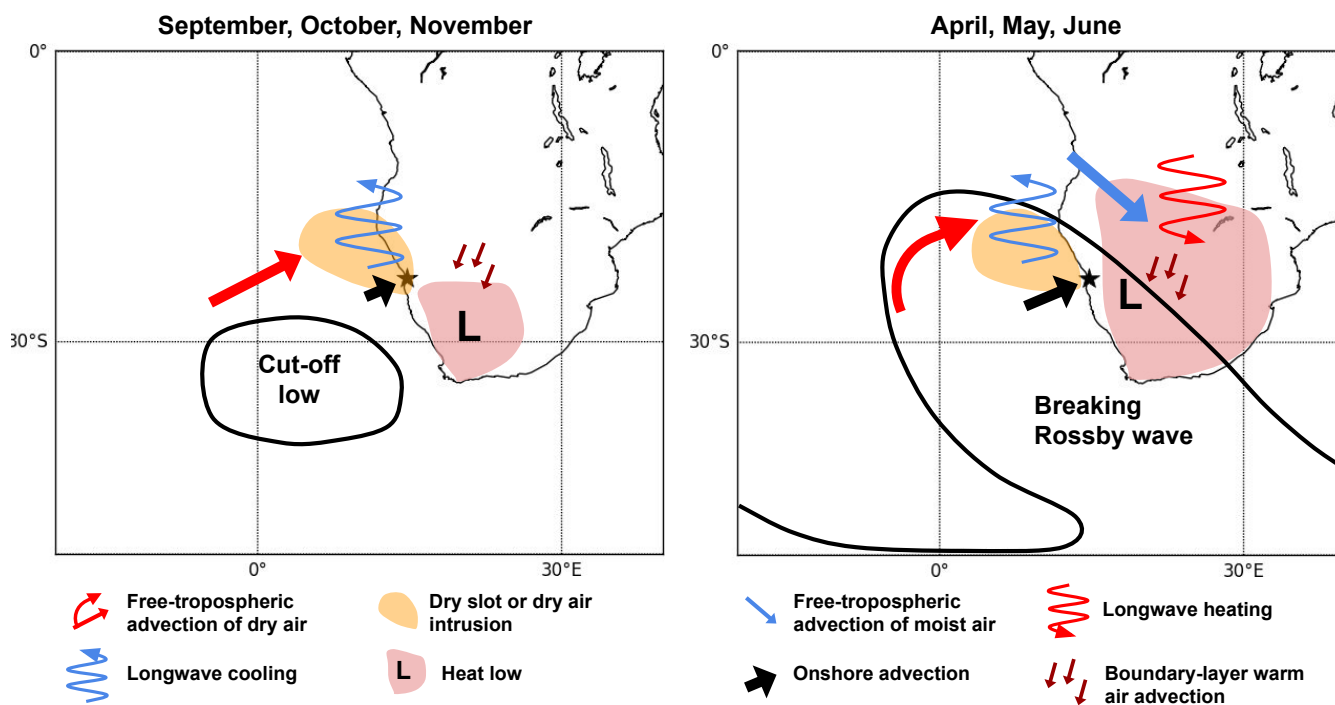
Figure 11. Schematic overview over the synoptical-scale mechanisms that modify day-to-day variability of central-Namib FLC occurrence during different seasons.

While it seems settled that, at least at the scales considered in this study, FLC occurrence is mostly driven by advective
5 processes, the quantitative contributions of humidity and temperature changes and radiative cooling for low-cloud formation in the Namib during the advection of marine boundary-layer air masses are still unclear. A heat budget analysis as in e.g., Adler et al. (2019) or Babić et al. (2019), based on ground-based measurements conducted during the field campaign of the Namib Life Cycle Analysis (NaFoLiCA) project (Spirig et al., 2019), is necessary to better understand the origin, development and life cycle of FLCs within the advected marine boundary-layer air masses. Future work should also focus on understanding
10 the local and possibly synoptic-scale drivers of the vertical structure of Namib-region FLCs on diurnal to seasonal scales, and the day-to-day variability of (marine) boundary-layer humidity. As FLCs in the Namib are clearly connected to marine stratus/stratocumulus clouds, findings of recent and ongoing field campaigns over the southeastern Atlantic (Zuidema et al., 2016; Formenti et al., 2019) and related insights concerning the aerosol-cloud-meteorology system of the Namibian stratocumulus cloud field (e.g., Adebiyi and Zuidema, 2018; Andersen and Cermak, 2015; Diamond et al., 2018; Formenti et al., 2019; Fuchs
15 et al., 2017, 2018; Gordon et al., 2018) are relevant to fully understand FLCs in the Namib desert.

Code and data availability. The ERA5 meteorological reanalysis data are freely available at the Copernicus Climate Change Service (C3S) Climate Date Store: https://cds.climate.copernicus.eu/#!/search?text=ERA5&type=dataset (last access: September 6th, 2019). Satellite data and code for data processing are available from the corresponding author upon reasonable request.

Appendix: Equations of statistical validation measures

5 $\quad$ POD $= \frac{a}{a+c}$

$\quad$ PC $= \frac{a+d}{a+b+c+d}$

$\quad$ FAR $= \frac{b}{a+b}$

$\quad$ CSI $= \frac{a}{a+b+c}$

$\quad$ BS $= \frac{a+b}{a+c}$

10 $\quad$ HSS $= \frac{2(ad-bc)}{(a+c)(c+d)+(a+b)(b+d)}$

$\quad$ with a = number of hits, b = number of false alarms, c = number of misses and d = number of correct negatives

Author contributions. HA and JC had the idea for the analysis. HA obtained and analyzed most of the data sets, conducted the original research and wrote the manuscript. JC and JF contributed to the study design, and JF computed initial backtrajectories. PK helped to develop a conceptual understanding of the synoptic-scale patterns and physical mechanisms. JQ computed the backtrajectories with Lagranto. MG
15 conducted the PCA analysis. SS contributed to the design of the statistical model, and RV contributed insights to local-scale processes. JC, JF, PK, JQ, MG, SS and RV contributed to manuscript preparation, and the interpretation of findings.

Competing interests. The authors declare that they have no conflict of interest.

Acknowledgements. Funding for this study was provided by Deutsche Forschungsgemeinschaft (DFG) in the project Namib Fog Life Cycle Analysis (NaFoLiCA), CE 163/7-1. HA acknowledges receiving a Research Travel Grant by the Karlsruhe House of Young Scientists
20 that supported a stay at ETH Zürich and thus facilitated the collaboration with SS. The contribution of JQ was funded by the Helmholtz Association (grant VH-NG-1243) MG was supported by the French National Research Agency under grant agreement no ANR-15-CE01-0014-01 (AEROCLO-sA).

References

Adebiyi, A. A. and Zuidema, P.: Low cloud cover sensitivity to biomass-burning aerosols and meteorology over the southeast Atlantic, Journal of Climate, 2, https://doi.org/10.1175/JCLI-D-17-0406.1, 2018.

Adler, B., Kalthoff, N., Lohou, F., Lothon, M., Dione, C., Pedruzo-bagazgoitia, X., and Andersen, H.: Nocturnal low-level clouds in the atmospheric boundary layer over southern West Africa: an observation-based analysis of conditions and processes, Atmospheric Chemistry and Physics, 19, 663–681, https://doi.org/10.5194/acp-19-663-2019, https://doi.org/10.5194/acp-19-663-2019, 2019.

Andersen, H. and Cermak, J.: How thermodynamic environments control stratocumulus microphysics and interactions with aerosols, Environmental Research Letters, 10, 24 004, https://doi.org/10.1088/1748-9326/10/2/024004, http://dx.doi.org/10.1088/1748-9326/10/2/024004, 2015.

Andersen, H. and Cermak, J.: First fully diurnal fog and low cloud satellite detection reveals life cycle in the Namib, Atmospheric Measurement Techniques, 11, 5461–5470, https://doi.org/10.5194/amt-11-5461-2018, https://www.atmos-meas-tech-discuss.net/amt-2018-213/, 2018.

Andersen, H., Cermak, J., Fuchs, J., Knutti, R., and Lohmann, U.: Understanding the drivers of marine liquid-water cloud occurrence and properties with global observations using neural networks, Atmospheric Chemistry and Physics, 17, https://doi.org/10.5194/acp-17-9535-2017, 2017.

Andersen, H., Cermak, J., Solodovnik, I., Lelli, L., and Vogt, R.: Spatiotemporal dynamics of fog and low clouds in the Namib unveiled with ground- and space-based observations, Atmospheric Chemistry and Physics, 19, 4383–4392, https://doi.org/10.5194/acp-19-4383-2019, https://doi.org/10.5194/acp-19-4383-2019, 2019.

Babić, K., Adler, B., Kalthoff, N., Andersen, H., Dione, C., Lohou, F., Lothon, M., and Pedruzo-bagazgoitia, X.: The observed diurnal cycle of low-level stratus clouds over southern West Africa: a case study, Atmospheric Chemistry and Physics, 19, 1281–1299, https://doi.org/10.5194/acp-19-1281-2019, https://doi.org/10.5194/acp-19-1281-2019, 2019.

Bendix, J., Eugster, W., and Klemm, O.: FOG – BOON OR BANE?, Erdkunde, 65, 229–232, http://www.jstor.org/stable/23069695, 2011.

Browning, K. A.: The dry intrusion perspective of extra-tropical cyclone development, Meteorological Applications, 324, 317–324, https://doi.org/10.1017/S1350482797000613, 1997.

Cermak, J.: Low clouds and fog along the South-Western African coast - Satellite-based retrieval and spatial patterns, Atmospheric Research, 116, 15–21, https://doi.org/10.1016/j.atmosres.2011.02.012, http://linkinghub.elsevier.com/retrieve/pii/S0169809511000615, 2012.

Deaconu, L. T., Ferlay, N., Waquet, F., Peers, F., Thieuleux, F., and Goloub, P.: Satellite inference of water vapor and aerosol-above-cloud combined effect on radiative budget and cloud top processes in the Southeast Atlantic Ocean, Atmospheric Chemistry and Physics Discussions, pp. 1–34, 2019.

Dee, D. P., Uppala, S. M., Simmons, A. J., Berrisford, P., Poli, P., Kobayashi, S., Andrae, U., Balmaseda, M. A., Balsamo, G., Bauer, P., Bechtold, P., Beljaars, A. C. M., van de Berg, L., Bidlot, J., Bormann, N., Delsol, C., Dragani, R., Fuentes, M., Geer, A. J., Haimberger, L., Healy, S. B., Hersbach, H., Hólm, E. V., Isaksen, L., Kållberg, P., Köhler, M., Matricardi, M., McNally, A. P., Monge-Sanz, B. M., Morcrette, J.-J., Park, B.-K., Peubey, C., de Rosnay, P., Tavolato, C., Thépaut, J.-N., and Vitart, F.: The ERA-Interim reanalysis: configuration and performance of the data assimilation system, Quarterly Journal of the Royal Meteorological Society, 137, 553–597, https://doi.org/10.1002/qj.828, http://doi.wiley.com/10.1002/qj.828, 2011.

Del Río, C., Garcia, J. L., Osses, P., Zanetta, N., Lambert, F., Rivera, D., Siegmund, A., Wolf, N., Cereceda, P., Larraín, H., and Lobos, F.: ENSO influence on coastal fog-water yield in the Atacama Desert, Chile, Aerosol and Air Quality Research, 18, 127–144, https://doi.org/10.4209/aaqr.2017.01.0022, 2018.

Deloncle, A., Berk, R., D'Andrea, F., and Ghil, M.: Weather Regime Prediction Using Statistical Learning, Journal of the Atmospheric Sciences, 64, 1619–1635, https://doi.org/10.1175/JAS3918.1, 2007.

Diamond, M. S., Dobracki, A., Freitag, S., Griswold, J. D. S., Heikkila, A., Howell, S. G., Kacarab, M. E., Podolske, J. R., Saide, P. E., and Wood, R.: Time-dependent entrainment of smoke presents an observational challenge for assessing aerosol – cloud interactions over the southeast Atlantic Ocean, Atmospheric Chemistry and Physics, 18, 14 623–14 636, https://doi.org/10.5194/acp-18-14623-2018, 2018.

Ebner, M., Miranda, T., and Roth-Nebelsick, A.: Efficient fog harvesting by Stipagrostis sabulicola (Namib dune bushman grass), Journal of Arid Environments, 75, 524–531, https://doi.org/10.1016/j.jaridenv.2011.01.004, http://www.sciencedirect.com/science/article/pii/S0140196311000061, 2011.

Eckardt, F., Soderberg, K., Coop, L., Muller, A., Vickery, K., Grandin, R., Jack, C., Kapalanga, T., and Henschel, J.: The nature of moisture at Gobabeb, in the central Namib Desert, Journal of Arid Environments, 93, 7–19, https://doi.org/10.1016/j.jaridenv.2012.01.011, http://www.sciencedirect.com/science/article/pii/S0140196312000432, 2013.

Formenti, P., Piketh, S. J., Namwoonde, A., Klopper, D., Burger, R., Cazaunau, M., Feron, A., Gaimoz, C., Broccardo, S., Walton, N., Desboeufs, K., Siour, G., Hanghome, M., Mafwila, S., Omoregie, E., Junkermann, W., and Maenhaut, W.: Three years of measurements of light-absorbing aerosols over coastal Namibia: seasonality, origin, and transport, Atmospheric Chemistry and Physics, 18, 17 003–17 016, https://doi.org/10.5194/acp-18-17003-2018, https://doi.org/10.5194/acp-18-17003-2018, 2018.

Formenti, P., D'Anna, B., Flamant, C., Mallet, M., Piketh, S. J., Schepanski, K., Waquet, F., Auriol, F., Brogniez, G., Burnet, F., Chaboureau, J.-P., Chauvigné, A., Chazette, P., Denjean, C., Desboeufs, K., Doussin, J.-F., Elguindi, N., Feuerstein, S., Gaetani, M., Giorio, C., Klopper, D., Mallet, M. D., Nabat, P., Monod, A., Solmon, F., Namwoonde, A., Chikwililwa, C., Mushi, R., Welton, E. J., and Holben, B.: The Aerosols, Radiation and Clouds in southern Africa (AEROCLO-sA) field campaign in Namibia: overview, illustrative observations and way forward, Bulletin of the American Meteorological Society, 0, null, https://doi.org/10.1175/BAMS-D-17-0278.1, https://doi.org/10.1175/BAMS-D-17-0278.1, 2019.

Friedman, J.: Fast sparse regression and classification, International Journal of Forecasting, 28, 722–738, https://doi.org/10.1016/j.ijforecast.2012.05.001, 2012.

Friedman, J., Hastie, T., and Tibshirani, R.: Regularization Paths for Generalized Linear Models via Coordinate Descent, Journal of Statistical Software, 33, 1–22, 2010.

Fuchs, J., Cermak, J., Andersen, H., Hollmann, R., and Schwarz, K.: On the Influence of Air Mass Origin on Low-Cloud Properties in the Southeast Atlantic, Journal of Geophysical Research: Atmospheres, 122, 11,076–11,091, https://doi.org/10.1002/2017JD027184, 2017.

Fuchs, J., Cermak, J., and Andersen, H.: Building a cloud in the Southeast Atlantic: Understanding low-cloud controls based on satellite observations with machine learning, Atmospheric Chemistry and Physics, 18, 16 537–16 552, https://doi.org/10.5194/acp-2018-593, 2018.

Garstang, M., Tyson, P. D., Swap, R., Edwards, M., Kållberg, P., and Lindesay, J. A.: Horizontal and vertical transport of air over southern Africa, Journal of Geophysical Research: Atmospheres, 101, 23 721–23 736, https://doi.org/10.1029/95JD00844, http://doi.wiley.com/10.1029/95JD00844, 1996.

Goldreich, Y. and Tyson, P. D.: Diurnal and Inter-Diurnal Variations in Large-Scale Atmospheric Turbulence Over Southern Africa, South African Geographical Journal, 70, 48–56, https://doi.org/10.1080/03736245.1988.10559755, 1988.

Gordon, H., Field, P. R., Abel, S. J., Johnson, B. T., Dalvi, M., Grosvenor, D. P., Hill, A. A., Miltenberger, A. K., Yoshioka, M., and Carslaw, K. S.: Large simulated radiative effects of smoke in the south-east Atlantic, Atmospheric Chemistry and Physics, 18, 15 261–15 289, https://doi.org/10.5194/acp-18-15261-2018, https://www.atmos-chem-phys-discuss.net/acp-2018-305/, 2018.

Gottlieb, T. R., Eckardt, F. D., Venter, Z. S., and Cramer, M. D.: The contribution of fog to water and nutrient supply to Arthraerua leubnitziae in the central Namib Desert, Namibia, Journal of Arid Environments, 161, 35–46, https://doi.org/10.1016/j.jaridenv.2018.11.002, https://doi.org/10.1016/j.jaridenv.2018.11.002, 2019.

Gultepe, I., Tardif, R., Michaelides, C., Cermak, J., Bott, A., Bendix, J., Müller, M. D., Pagowski, M., Hansen, B., Ellrod, G., Jacobs, W., Toth, G., and Cober, S. G.: Fog Research: A Review of Past Achievements and Future Perspectives, Pure and Applied Geophysics, 164, 1121–1159, https://doi.org/10.1007/s00024-007-0211-x, 2007.

Haensler, A., Cermak, J., Hagemann, S., and Jacob, D.: Will the southern african west coast fog be affected by future climate change?: Results of an initial fog projection using a regional climate model, Erdkunde, 65, 261–275, https://doi.org/10.3112/erdkunde.2011.03.04, 2011.

Hastie, T., Tibshirani, R., and Friedman, J.: The Elements of Statistical Learning, Springer Series in Statistics New York, NY, USA, 2nd edn., 2001.

Henschel, J. R., Wassenaar, T. D., Kanandjembo, A., Louw, M. K., Neef, G., Shuuya, T., and Soderberg, K.: Roots point to water sources of <i>Welwitschia mirabilis</i> in a hyperarid desert, Ecohydrology, p. e2039, https://doi.org/10.1002/eco.2039, http://doi.wiley.com/10.1002/eco.2039, 2018.

Hersbach, H.: The ERA5 Atmospheric Reanalysis., AGU Fall Meeting Abstracts, 2016.

Jackson, S. P.: A Note on the Climate of Walvis Bay, South African Geographical Journal, 23, 46–53, https://doi.org/10.1080/03736245.1941.10559213, 1941.

James, R. and Washington, R.: Changes in African temperature and precipitation associated with degrees of global warming, Climatic Change, 117, 859–872, https://doi.org/10.1007/s10584-012-0581-7, 2013.

Kaseke, K. F., Wang, L., and Seely, M. K.: Nonrainfall water origins and formation mechanisms, Science Advances, 3, e1603 131, https://doi.org/10.1126/sciadv.1603131, http://advances.sciencemag.org/lookup/doi/10.1126/sciadv.1603131, 2017.

Kaseke, K. F., Tian, C., Wang, L., Seely, M., Vogt, R., Wassenaar, T., and Mushi, R.: Fog spatial distributions over the central Namib Desert - An isotope approach, Aerosol and Air Quality Research, 18, 49–61, https://doi.org/10.4209/aaqr.2017.01.0062, 2018.

Klein, S. A. and Hartmann, D. L.: The Seasonal Cycle of Low Stratiform Clouds, Journal of Climate, 6, 1587–1606, https://doi.org/10.1175/1520-0442(1993)006<1587:TSCOLS>2.0.CO;2, 1993.

Knippertz, P. and Martin, J. E.: Tropical plumes and extreme precipitation in subtropical and tropical West Africa, Quarterly Journal of the Royal Meteorological Society, 131, 2337–2365, https://doi.org/10.1256/qj.04.148, http://www.nature.com/doifinder/10.1038/nclimate2727, 2005.

Lancaster, J., Lancaster, N., and Seely, M. K.: Climate of the central Namib desert, Madoqua, 14, 5–61, 1984.

Lindesay, J. A. and Tyson, P. D.: Climate and Near-surface Airflow Over the Central Namib, in: Namib Ecology: 25 years of Namib research, 7, pp. 27–37, Transvaal Museum, Pretoria, 1990.

Maúre, G., Pinti, I., Ndebele-Murisa, M., Muthige, M., Lennard, C., Nikulin, G., Dosio, A., and Meque, A.: The southern African climate under 1.5 °C and 2 °C of global warming as simulated by CORDEX regional climate models, Environmental Research Letters, 13, https://doi.org/10.1088/1748-9326/aab190, https://doi.org/10.1088/1748-9326/aab190, 2018.

Nagel, J. F.: Fog Precipitation at Swakopmund, South African Weather Bureau Newsletter, 125, 1–9, 1959.

Ndarana, T. and Waugh, D. W.: The link between cut-off lows and Rossby wave breaking in the Southern Hemisphere, Quarterly Journal of the Royal Meteorological Society, 136, 869–885, https://doi.org/10.1002/qj.627, 2010.

Nicholson, S. E.: A low-level jet along the Benguela coast, an integral part of the Benguela current ecosystem, Climatic Change, 99, 613–624, https://doi.org/10.1007/s10584-009-9678-z, 2010.

5 Olivier, J.: Spatial distribution of fog in the Namib, Journal of Arid Environments, 29, 129–138, https://doi.org/10.1016/S0140-1963(05)80084-9, http://linkinghub.elsevier.com/retrieve/pii/S0140196305800849, 1995.

Olivier, J. and Stockton, P. L.: The influence of upwelling extent upon fog incidence at Lüderitz, southern Africa, International Journal of Climatology, 9, 69–75, https://doi.org/10.1002/joc.3370090106, 1989.

Pedregosa, F., Varoquaux, G., Gramfort, A., Michel, V., Thirion, B., Grisel, O., Blondel, M., Louppe, G., Prettenhofer, P., Weiss, R., Dubourg,
10 V., Vanderplas, J., Passos, A., Cournapeau, D., Brucher, M., Perrot, M., and Duchesnay, É.: Scikit-learn: Machine Learning in Python, Journal of Machine Learning Research, 12, 2825–2830, https://doi.org/10.1007/s13398-014-0173-7.2, http://dl.acm.org/citation.cfm?id=2078195{%}5Cnhttp://arxiv.org/abs/1201.0490http://arxiv.org/abs/1201.0490, 2011.

Roth-Nebelsick, A., Ebner, M., Miranda, T., Gottschalk, V., Voigt, D., Gorb, S., Stegmaier, T., Sarsour, J., Linke, M., and Konrad, W.: Leaf surface structures enable the endemic Namib desert grass Stipagrostis sabulicola to irrigate itself with fog water., Journal of the Royal So-
15 ciety, Interface / the Royal Society, 9, 1965–74, https://doi.org/10.1098/rsif.2011.0847, http://www.pubmedcentral.nih.gov/articlerender.fcgi?artid=3385753{&}tool=pmcentrez{&}rendertype=abstract, 2012.

Schmetz, J., Pili, P., Tjemkes, S., Just, D., Kerkmann, J., Rota, S., and Ratier, A.: An Introduction to Meteosat Second Generation (MSG), Bulletin of the American Meteorological Society, 83, 977–992, https://doi.org/110.1175/BAMS-83-7-Schmetz-1, 2002.

Seely, M. K.: Irregular fog as a water source for desert dune beetles, Oecologia, 42, 213–227, https://doi.org/10.1007/BF00344858, http:
20 //www.springerlink.com/content/x34r526hn5075653, 1979.

Seely, M. K. and Henschel, J. R.: The Climatology of Namib Fog, Proceedings, First International Conference on Fog and Fog Collection, Vancouver, Canada, pp. 353–356, 1998.

Seely, M. K., De-Vos, M. P., and Louw, G. N.: Fog imbibition satellite fauna and unusual leaf structure in a namib desert dune plant trianthema hereroensis, South African Journal of Science, 73, 169–172, 1977.

25 Sippel, S., Meinshausen, N., Merrifield, A., Lehner, F., Pendergrass, A. G., Fischer, E., and Knutti, R.: Uncovering the forced climate response from a single ensemble member using statistical learning, Journal of Climate, 0, null, https://doi.org/10.1175/JCLI-D-18-0882.1, https://doi.org/10.1175/JCLI-D-18-0882.1, 2019.

Spirig, R., Vogt, R., Larsen, J. A., Feigenwinter, C., Wicki, A., Parlow, E., Adler, B., Kalthoff, N., Cermak, J., Andersen, H., Fuchs, J., Bott, A., Hacker, M., Wagner, N., Maggs-Kölling, G., Wassenaar, T., and Seely, M.: Probing the fog life-cycles in the Namib desert, Bulletin of
30 the American Meteorological Society, https://doi.org/10.1175/BAMS-D-18-0142.1, 2019.

Sprenger, M. and Wernli, H.: The LAGRANTO Lagrangian analysis tool – version 2.0, Geoscientific Model Development, 8, 2569–2586, https://doi.org/10.5194/gmd-8-2569-2015, 2015.

Storch, H. v. and Zwiers, F. W.: Statistical Analysis in Climate Research, Cambridge University Press, https://doi.org/10.1017/CBO9780511612336, 1999.

35 Swap, R. J., Annegarn, H. J., Suttles, J. T., King, M. D., Platnick, S., Privette, J. L., and Scholes, R. J.: Africa burning: A thematic analysis of the Southern African Regional Science Initiative (SAFARI 2000), Journal of Geophysical Research - Atmospheres, 108, 1–15, https://doi.org/10.1029/2003JD003747, 2003.

Tyson, P. D., Garstang, M., Swap, R. J., Kallberg, P., and Edwards, M.: An Air Transport Climatology for Subtropical Southern Africa, International Journal of Climatology, 16, 265–291, https://doi.org/10.1002/(SICI)1097-0088(199603)16, 1996.

Warren-Rhodes, K. A., Mckay, C. P., Boyle, L. N., Wing, M. R., Kiekebusch, E. M., Cowan, D. A., Stomeo, F., Pointing, S. B., Kaseke, K. F., Eckardt, F., Henschel, J. R., Anisfeld, A., Seely, M., and Rhodes, K. L.: Physical ecology of hypolithic communities in the cen-

5   tral Namib Desert: The role of fog, rain, rock habitat, and light, Journal of Geophysical Research: Biogeosciences, 118, 1451–1460, https://doi.org/10.1002/jgrg.20117, 2013.

Yu, J.-Y. and Kim, S. T.: Relationships between Extratropical Sea Level Pressure Variations and the Central Pacific and Eastern Pacific Types of ENSO, Journal of Climate, 24, 708–720, https://doi.org/10.1175/2010JCLI3688.1, 2010.

Zhou, C. and Penner, J. E.: Why do general circulation models overestimate the aerosol cloud lifetime effect? A case study comparing CAM5

10   and a CRM, Atmospheric Chemistry and Physics, 17, 21–29, https://doi.org/10.5194/acp-17-21-2017, 2017.

Zuidema, P., Redemann, J., Haywood, J., Wood, R., Piketh, S., Hipondoka, M., Formenti, P., Zuidema, P., Redemann, J., Haywood, J., Wood, R., Piketh, S., Hipondoka, M., and Formenti, P.: Smoke and Clouds above the Southeast Atlantic: Upcoming Field Campaigns Probe Absorbing Aerosol's Impact on Climate, Bulletin of the American Meteorological Society, 97, 1131–1135, https://doi.org/10.1175/BAMS-D-15-00082.1, http://journals.ametsoc.org/doi/10.1175/BAMS-D-15-00082.1, 2016.